

40. B. M. Discher et al., *J. Phys. Chem. B* **106**, 2848 (2002).
41. C. Nardin, T. Hirt, J. Leukel, W. Meier, *Langmuir* **16**, 1035 (2000).
42. Polydispersities are generally reported as weight-average MW divided by number-average MW; typical ratios for the copolymers of Fig. 1 are ~1.05 to 1.15. A value of 1.7 was reported for the triblock copolymer of (41).
43. K. Schillen, K. Bryskhe, Y. S. Mel'nikova, *Macromolecules* **32**, 6885 (1999).
44. N. A. J. M. Sommerdijk, S. J. Holder, R. C. Hiorns, R. G. Jones, R. J. M. Nolte, *Macromolecules* **33**, 8289 (2000).
45. A. Napoli, N. Tirelli, G. Kilcher, J. A. Hubbell, *Macromolecules* **34**, 8913 (2001).
46. R. P. Batycky, J. Hanes, R. Langer, D. A. Edwards, *J. Pharm. Sci.* **86**, 1464 (1997).
47. S. A. Hagan et al., *Langmuir* **12**, 2153 (1996).
48. PEO-PLA vesicles have been observed with a copolymer having $f_{\text{PEO}} \approx 33\%$ and $MW \approx 6 \text{ kg/mol}$ (59).
49. R. Mathur, P. Capasso, *ACS Symp. Ser.* **610** (1995), p. 219.
50. J. M. Gebicki, M. Hicks, *Nature* **243**, 232 (1973).
51. M. Regenberg, S. Akari, S. Forster, H. Mohwald, *J. Phys. Chem. B* **103**, 6669 (1999).
52. F. Caruso, D. Trau, H. Mohwald, R. Renneberg, *Langmuir* **16**, 1485 (2000).
53. S. A. Jenekhe, X. L. Chen, *Science* **279**, 1903 (1998).
54. W. Meier, C. Nardin, M. Winterhalter, *Angew. Chem. Int. Ed.* **39**, 4599 (2000).
55. N. Dan, S. A. Safran, *Macromolecules* **27**, 5766 (1994).
56. A. Graff, M. Sauer, P. V. Gelder, W. Meier, *Proc. Natl. Acad. Sci. U.S.A.* **99**, 5064 (2002).
57. K. Velonia, A. E. Rowan, R. J. M. Nolte, *J. Am. Chem. Soc.* **124**, 4224 (2002).
58. E. Helfand, in *Developments in Block Copolymers*, Z. R. Wasserman, Ed. (Applied Science, New York, 1982), chapter 4.
59. F. Ahmed, I. Omaswa, A. Brannan, F. S. Bates, D. E. Discher, in preparation.
60. O. Lambert, L. Letellier, W. M. Gelbart, J.-L. Rigaud, *Proc. Natl. Acad. Sci. U.S.A.* **97**, 7248 (2000).
61. P. Photos, B. M. Discher, L. Bacakova, F. S. Bates, D. E. Discher, in preparation.
62. Support for our work and interest (D.E.D.) in polymer vesicles was provided by the NSF Materials Research Science and Engineering Center (MRSEC) at the University of Pennsylvania and by an NSF-PECASE award (D.E.D.).

REVIEW

How Surface Topography Relates to Materials' Properties

Hazel Assender, Valery Bliznyuk,* Kyriakos Porfyrakis

The topography of a surface is known to substantially affect the bulk properties of a material. Despite the often nanoscale nature of the surface undulations, the influence they have may be observed by macroscopic measurements. This review explores many of the areas in which the effect of topography is macroscopically relevant, as well as introducing some recent developments in topographic analysis and control.

Those few materials whose surface is atomically flat are of great use to scientists and for certain technological applications; however, the majority of materials have a surface landscape made up of undulations and even perhaps steep gradients and pores. These constitute the topography of the surface, a property that is often difficult to define by a few simple parameters but nevertheless can have a considerable impact on a material's performance. Such importance reflects the surface-specific nature of many properties: the ability to adhere to another material, optical properties, or tribology, for example.

Issues of topography are perhaps particularly pertinent in the case of soft matter. For instance, the size of typical topographic features may be comparable with the molecular dimension and, for some technologies, with the thickness of the soft layer itself. Soft matter allows the use of a number of specific methods to manipulate topography, and in the kinds of applications in which soft matter is employed, the topography is often of specific importance. For example, for food packaging, a compliant adhesive layer might be used to smooth the surface of a polymer substrate

before the deposition of a gas barrier layer (1). Similarly, the electro-optical behavior of thin films of polymers used in electronic devices has been shown to correlate with their topography (2, 3).

The correlation between surface structure and properties is important within two broad areas of considerable recent interest in materials science. The first is in the realm of biological and biomedical materials, in which the shape of a surface controls its interaction with biological components; for example, whether bacteria will grow on a particular surface—a subject of interest to anyone who wishes to keep surfaces hygienic or their teeth clean! The second important developing area is that of nanocomposites and nanostructured materials, which frequently combine soft matter with metals or ceramics for applications as diverse as electronics, packaging, and information storage. When combining materials on scales in the range from 10 nm to 1 μm (and these include many that are found in biology), the interface becomes of substantive importance to the materials' performance; and the topography of the interface, or the surface as a precursor to an interface, may be on a comparable scale to that of the nanostructured material.

The Origin of Topography

Topography may be induced at the surface of soft matter by its inherent relaxation or, more actively for example, by the exploitation of mixtures of materials, mechanical roughening, chemical patterning, or even electric fields.

When allowed to relax at its surface, soft matter will form surface undulations, known as capillary waves, as a result of the inherent entropy of the system balancing the increased energy of the greater surface area (4). The relatively low surface energy of molecular materials combined with their compliance makes such an effect important in soft materials. The addition of an electric field can lead to electrohydrodynamic instabilities and consequent patterning of a viscous polymer film (5).

One example is shown in Fig. 1, where a thin polystyrene film [capped with an ultrathin (flexible) Al layer as an electrode] has dewetted an Al-coated substrate after application of an electric field of strength $5.7 \times 10^7 \text{ V m}^{-1}$ (6). One possible application of layers that have artificially induced topography such as this might be the creation of antireflective coatings in which the roughened surface scatters the reflected light (7). Where block copolymers are used, such nanopatterning may be controlled by the phase structure resulting from two-dimensional (2D) viscous flow as the structure orders, and it also may be influenced by the topography of an underlying substrate (8). Electric fields may also influence the patterning formed in these copolymer systems (9). Similarly, thin films of blends may be exploited to produce a surface topography resulting from phase separation processes (10). In addition, chemical patterning of a surface may lead to preferential phase separation to induce nanopatterning in the topography of a subsequent layer (11). Many impressive structures have been reported, and the whole area of nanopatterning, nanolithography, and self-organizing layers is an area of current great excitement. We await further developments in the practical exploitation of such systems and in the degree to which they may be controlled on a more substantial scale.

Department of Materials, University of Oxford, Parks Road, Oxford OX1 3PH, UK.

*Present address: Department of Construction Engineering, Materials Engineering, and Industrial Design, Western Michigan University, Kalamazoo, MI 49008, USA.

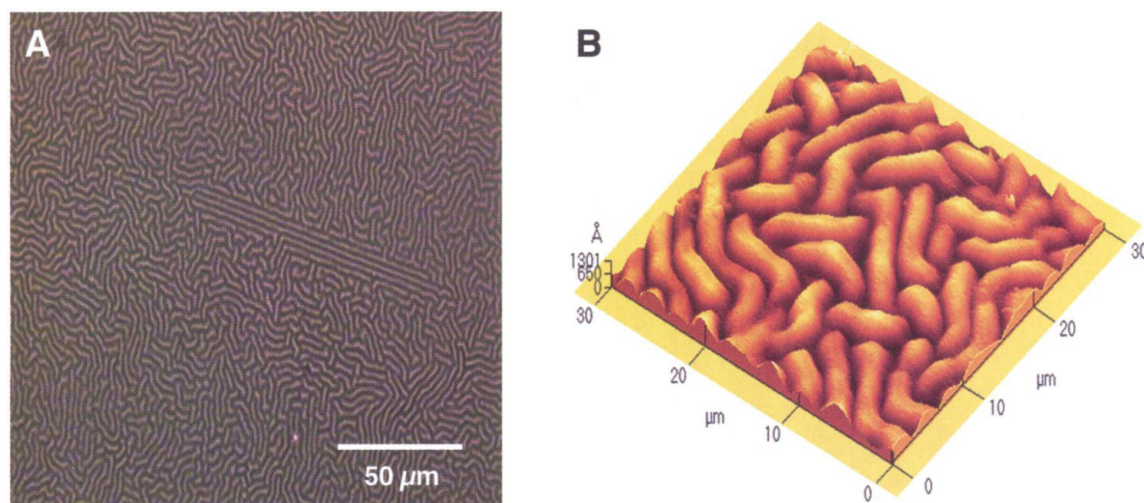


Fig. 1. (A) Reflection-mode optical micrograph of the lateral structure induced by an electric field applied across a polystyrene film capped by an Al layer acting as an electrode. The origin of the ordered region toward the center of the micrograph is currently under investigation. (B) AFM image taken using a tapping mode scan of the lateral morphology, showing the topography of the film surface. [Micrographs courtesy of S. Hutchinson and D. Bucknall]

In molecular matter, including polymers, the molecular size itself might be expected to influence the topography. Molecules will tend to coil into bundles with an associated radius of gyration, R_g , and even within an entangled system, the undulations that form on the surface of the material on molecular relaxation have been found to be associated with the molecular size (R_g) in both simulations and experimental measurements (12).

Where there is more than one phase at, or close to, the surface, the surface topography will be influenced by the multiple phases. One example of this is semicrystalline polymers. Figure 2 shows atomic force microscopy (AFM) images of a crystallizable polymer, poly(ethylene terephthalate) (PET), that has been spin-cast onto a glass substrate. The resulting amorphous surface is rather flat (Fig. 2A), but subsequent annealing to form the semicrystalline material results in distinct roughening of the surface (Fig. 2B) (13). The molecular rearrangement required for crystallization, coupled with the relatively rigid nature of the crystals themselves, give rise to the resulting topography. Very careful examination of biaxially drawn PET films (14) has revealed a comparable topography, with features in the surface profile that can be associated with crystals, although study of biaxially drawn PET with various force microscopies has given no evidence for the crystals directly penetrating the surface, suggesting that it is the subsurface that is controlling the topography in this case.

The effect of multiple phases is at least as important to the topography when inorganic material is mixed with a polymer to form a composite. The effect is exploited by users of AFM and scanning electron microscopy (SEM) to distinguish the phases in composite systems, although more definitive analysis may be made

by careful use of the microscopes to distinguish the phases using phenomena other than the topography, such as analysis of the backscattered electrons and the difference in fracture behavior in SEM, as well as the use of various oscillating tips or lateral force modes in scanning force microscopies.

It has long been established that the manner of processing will affect the surface finish of a component, in the more severe cases manifesting itself on a scale visible to the naked eye. The simplest case is perhaps one where the surface finish reflects the profile of a mould or die wall, but rheological effects such as the formation of "sharkskin" in extrusions are also of great importance. The considerable knowledge and experience of such phenomena are beyond the scope of this paper to discuss, but good reviews may be found elsewhere (15–18).

Topographic Analysis

The topography of a particular surface is measured by some kind of profilometry. This may be mechanical, in which a probe is passed

will not be deformed, but the applicability of this method depends on the surface reflectivity and the limit of the resolution of the radiation of choice.

Profilometry can generate an image of the surface height, but it is frequently important to extract some characteristic parameters to define the surface, and any number of analyses may be envisaged. In all cases, the value of any parameters will depend on the size of the area measured. Just as the size of a probe limits the size of small features that can be detected, if too small a sample area is studied, it is likely that features on the surface that are larger or have a large periodicity will be overlooked.

Perhaps the most frequently quoted parameter is the root mean square (rms) roughness (that is, the rms height of the surface around some mean value), but this does not take any account of the distance between the features on the surface; for example, a surface with a few high-amplitude features may have the same rms value as one with many low-lying features. Similarly, it does not reflect any anisotropy in

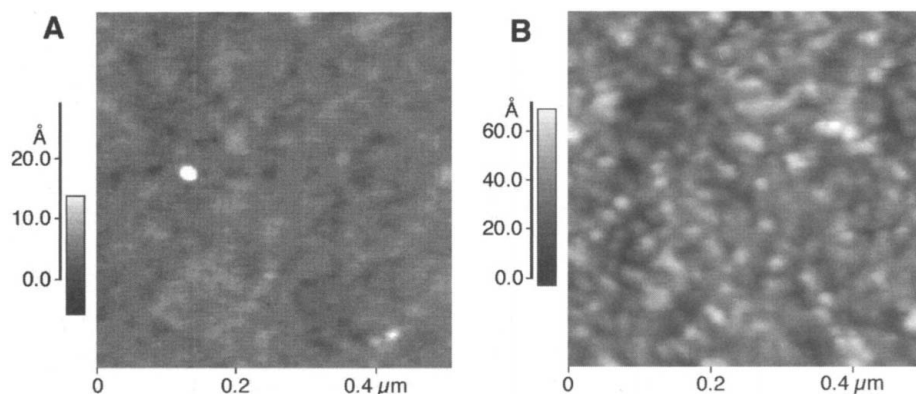


Fig. 2. AFM images of spin-coated PET film (A) before the annealing and (B) after 3 min of annealing at 95°C to increase the crystallinity. The surface roughness has increased with the change in crystallinity.

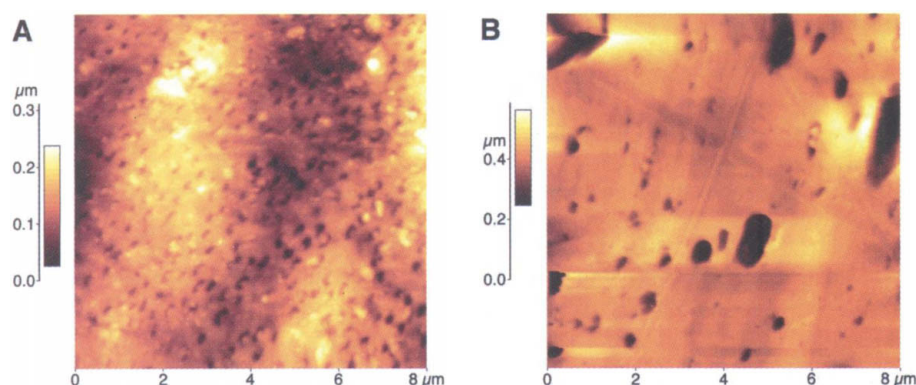


Fig. 3. AFM images of two polymer surfaces with very similar rms roughness but contrasting gloss. (A) Rubber-toughened acrylic, rms = 38.5 nm, gloss = 18.9%. (B) PVC, rms = 36.1 nm, gloss = 78.7%.

the topography. 2D analysis may be carried out by Fourier transform (FT) analysis, for example, but a 2D autocorrelation function (ACF) (19) has been found to be preferred for amorphous systems. FT or ACF analyses will characterize the surface more fully than the rms value. The 2D ACF is given by

$$\text{ACF}(x, y) = \frac{\iint \rho(x - x', y - y') \times \rho(x', y') dx' dy'}{\iint \rho^2(x, y) dx dy} \quad (1)$$

where $\rho(x, y)$ is a profile function defined on the surface (x, y) , and the denominator is a normalization factor. It thus compares the height at point (x, y) with that at some second point (x', y') and maps this comparison as a function of the distance between them. Thus, the initial decay (which might be fitted to an exponential function to give a characteristic correlation length, ξ_1) in the ACF reflects any local short-range correlation in the structure, and any undulations in the surface with an approximately uniform spacing will give rise to oscillations in the ACF. The first maximum in the ACF will be at a length associated with the distance between features in the topography (20). Assuming that the topography is not totally regular, these oscillations will decay with distance $[(x^2 + y^2)^{0.5}]$, leading to a second correlation length, ξ_2 . Such analysis has been applied to a study of the roughness of polystyrene after molecular relaxation on annealing (12), and it showed good agreement with computer simulation results and a correlation between the radius of gyration of the molecule and ξ_2 .

Other related analyses have included Fourier index analysis (21), giving a power spectrum of the frequency with which features of a certain size appear in the topography, and fractal analysis, which considers the importance of the scale of measurement with regard to the structural characteristics: the rms height obtained at several different “magnifications” of the AFM versus scan size on a double logarithmic scale is linear for a fractal surface with a fractal dimension that depends on the gradient (20, 22).

Properties

Adhesion. The ability of one surface to adhere to another depends on a number of factors, such as the degree of chemical interaction between the two components, the proximity, and the area of contact. For the latter two factors, there is clearly a dependence on the topography of the surfaces to be joined. Correlation between the fractal properties of the surface and the adhesion strength has been demonstrated for polymer composites. If some kind of adhesive or coating is to be used that is applied as a liquid or semisolid, the degree to which the adhesive may spread across the surface and fill the crevices of the surface will depend on the interfacial energies and the topography of the solid surface(s). Thus, the preparation of a surface for bonding is found to be of crucial importance to effect a good macroscopic bond. There are two primary goals of good surface preparation: removal or introduction of chemical species for improved chemical interaction (such as cleaning the surface of grease spots, plasma, or corona discharge treatments) and roughening the surface to the correct degree. Treatments such as plasmas (23, 24), corona discharge (25), ultraviolet exposure (26), or photochemical reaction (27) are also thought to play a role in roughening the surface.

Gloss. The optical finish or gloss of a surface is directly linked to its topography. Gloss has been described as a geometric attribute of surfaces that “causes them to have a shiny or lustrous appearance” (28). A surface’s gloss is considered to be the proportion of incident light that is reflected at the specular reflectance angle of the mean plane of that surface. The local specular

reflectance for unpolarized light, R_s , is predicted from the Fresnel formula

$$R_s = \frac{1}{2} \left[\left(\frac{\cos i - \sqrt{n^2 - \sin^2 i}}{\cos i + \sqrt{n^2 - \sin^2 i}} \right)^2 + \left(\frac{n^2 \cos i - \sqrt{n^2 - \sin^2 i}}{n^2 \cos i + \sqrt{n^2 - \sin^2 i}} \right)^2 \right] \quad (2)$$

where n is the sample refractive index and i is the angle of incidence. Thus, variations in refractive index in the plane of the surface and the topography (and hence the local angles of incidence) both affect the gloss.

The conventional wisdom that resulted from early work on gloss (29) led to the overall rms roughness (σ) being related directly to the gloss of a surface (the relative reflectance R)

$$R = \exp \left\{ - \left(\frac{4\pi\sigma \cos i}{\lambda} \right)^2 \right\} \quad (3)$$

where i is the angle of incidence of the gloss measurement and λ is the wavelength of incident light. This relation has since been extensively quoted and applied (30–32). However, it does not take into account in-plane distribution of the various undulations of the surface, which necessarily determines the light scattering, particularly where the spacings are comparable to the wavelength of the incident light. One example where the measured gloss of the surface is not directly related to the rms roughness is given in Fig. 3, as the two surfaces shown have very similar rms roughness values but very different gloss (33).

A more rigorous analysis of surface scattering of light has been made by Whitehouse, who considered the case of diamond-machined steel surfaces (34). For a 1D case, the scattered intensity $I(\omega)$ is expressed in terms of the autocorrelation function $A(\tau)$ of the surface

$$I(\omega) = R^2 \exp[-k^2 \sigma^2 (1 - A(\tau))] \exp \left(- \frac{jk\omega\tau}{f} \right) d\tau \quad (4)$$

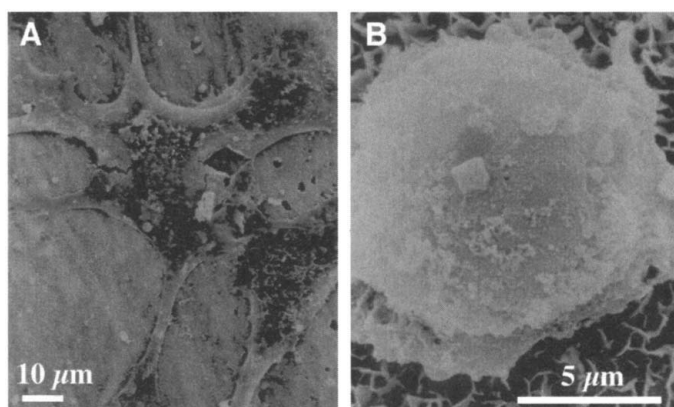


Fig. 4. Scanning electron micrographs of (A) a polygonal osteoblast and (B) a spheroidal osteoblast on octacalcium phosphate-coated collagen. [Micrographs courtesy of A. Lawson and J. Czernuszka]

where R is the reflectance of the sample, τ is the distance on the surface between two points, ω is the angular frequency, k is the wave number, f is the focal length of the incident radiation, and σ is the rms height of the surface. A 2D analysis of the optics has been carried out by Ogilvy (35). Whitehouse concluded (34) (for undulations with length scale greater than the wavelength of the incident radiation) that the surface appeared glossy if the probability density of the slopes on the surface was strictly confined to a narrow angle.

Biocompatibility. Finally, biological interactions with a surface have also been found to depend on its topography. A good review of the topological control of cell adhesion and activity on a surface has been made by Curtis and Wilkinson (36), and a more general review of the role of polymer biomaterials may also be found (37). Such considerations are relevant for a number of in vivo and in vitro applications, such as biological sensors, hip replacements (38), and more complex tissue implants such as replacement bone, where the growth of cells within the artificial structure is to be encouraged. For example, the size and morphology of crystals at the surface of octacalcium phosphate-coated collagen have been shown to affect the interaction of cells with the surface, as illustrated in Fig. 4. The larger scale topography was found to lead to less favorable spheroidal cells that formed fewer intercellular connections (39). In some cases, the topography of a surface may be carefully controlled to promote cell adhesion (40, 41).

Conclusion

The topography of a surface is a direct result of the nature of the material that defines it.

The analysis of the topography of a sample, made possible on the nanoscale by the development of AFM techniques, needs to be carefully considered in order to relate the complexity of a 2D surface to the material's properties. The result will be the better control of a number of properties, such as optical finish, and of the interaction of a surface with a secondary material, whether that be an adhesive, a secondary component of a composite, or a biological species.

References and Notes

1. J. D. Affinito et al., *Thin Solid Films* **291**, 63 (1996).
2. J. A. DeAro, K. D. Weston, S. K. Buratto, U. Lemmer, *Chem. Phys. Lett.* **277**, 532 (1997).
3. Y. Nabetani, M. Yamasaki, A. Miura, N. Tamai, *Thin Solid Films* **393**, 329 (2001).
4. M. Sferazza et al., *Phys. Rev. Lett.* **78**, 3693 (1997).
5. E. Schäffer, T. Thurn-Albrecht, T. P. Russell, U. Steiner, *Europhys. Lett.* **53**, 218 (2001).
6. D. G. Bucknall, G. A. D. Briggs, *MRS Symp. Ser.: Nanopatterning: Ultralarge-Scale Integration Biotechnol.* **705**, 151 (2002), L. Merhari, K. E. Gonsalves, E. A. Dobisz, M. Angelopoulos, D. Herr, Eds.
7. S. Walheim, E. Schäffer, J. Mlynek, U. Steiner, *Science* **283**, 520 (1999).
8. J. Heier, E. Sivanah, E. J. Kramer, *Macromolecules* **32**, 9007 (1999).
9. T. Thurn-Albrecht, J. DeRouchey, T. P. Russell, *Macromolecules* **33**, 3250 (2000).
10. A. Karim et al., *Macromolecules* **31**, 857 (1998).
11. X. P. Jiang, H. P. Zheng, S. Gourdin, P. T. Hammond, *Langmuir* **18**, 2607 (2002).
12. G. Goldbeck-Wood et al., *Macromolecules* **35**, 5283 (2002).
13. V. N. Bliznyuk, K. Kirov, H. E. Assender, G. A. D. Briggs, *Polym. Preprints* **41**, 1489 (2000).
14. F. Dinelli, H. E. Assender, K. Kirov, O. V. Kolosov, *Polymer* **41**, 4285 (2000).
15. C. Rauwendaal, *Polymer Extrusion* (Hanser, Munich, 1985).
16. S.-J. Liu, *Plast. Rubber Composites* **30**, 170 (2001).
17. B. Monasse et al., *Plast. Elastomers Mag.* **53**, 29 (2001).
18. Y. Oyanagi, *Int. Polym. Sci. Technol.* **24**, T38 (1997).
19. A. Guinier, *X-ray Diffraction in Crystals, Imperfect Crystals, and Amorphous Bodies* (W. H. Freeman, San Francisco, 1963).
20. V. N. Bliznyuk, V. M. Burlakov, H. E. Assender, G. A. D. Briggs, Y. Tsukahara, *Macromol. Symp.* **167**, 89 (2001).
21. W. M. Tong, R. S. Williams, *Annu. Rev. Phys. Chem.* **45**, 401 (1994).
22. P. Meakin, *Fractals, Scaling and Growth Far from Equilibrium* (Cambridge Univ. Press, Cambridge, 1998).
23. C. M. Chan, T. M. Ko, H. Hiraoka, *Surf. Sci. Rep.* **24**, 3 (1996).
24. E. M. Liston, L. Martinu, M. R. Wertheimer, *J. Adhesion Sci. Technol.* **7**, 1091 (1993).
25. Q. C. Sun, D. D. Zhang, L. C. Wadsworth, *Tappi J.* **81**, 177 (1998).
26. V. Bliznyuk et al., *Macromolecules* **32**, 361 (1999).
27. N. Zettsu, T. Ubukata, T. Seki, K. Ichimura, *Adv. Mater.* **13**, 1693 (2001).
28. R. S. Hunter, R. W. Harold, *The Measurement of Appearance* (Wiley, New York, ed. 2, 1987).
29. H. Davies, *Proc. Inst. Electr. Eng.* **101**, 209 (1954).
30. F. M. Willmouth, in *Optical Properties of Polymers*, G. H. Meeten, Ed. (Elsevier, Amsterdam, 1986).
31. D. Porter, *Group Interaction Modelling of Polymer Properties* (Marcel Dekker, New York, 1995).
32. P. Beckmann, A. Spizzichino, *The Scattering of Electromagnetic Waves from Rough Surfaces* (Pergamon, New York, 1987).
33. K. Porfyrakis, N. Marston, H. E. Assender, in preparation.
34. D. J. Whitehouse, *Proc. Inst. Mech. Eng. B: J. Eng. Manuf.* **207**, 31 (1993).
35. J. A. Ogilvy, *Theory of Wave Scattering from Random Rough Surfaces* (Adam Hilger, Bristol, UK, 1991).
36. A. Curtis, C. Wilkinson, *Biomaterials* **18**, 1573 (1997).
37. L. G. Griffith, *Acta Mater.* **48**, 263 (2000).
38. T. M. McCloughlin, A. G. Kavanagh, *Proc. Inst. Mech. Eng. Part H-J. Eng. Med.* **214**, 349 (2000).
39. A. C. Lawson et al., *MRS Symp. Ser.: Biomed. Mater.: Drug Delivery, Implants Tissue Eng.* **550**, 235 (1999), T. Neenan, M. Marcolongo, R. F. Valentini, Eds.
40. C. S. Ranucci, P. V. Moghe, *J. Biomed. Mater. Res.* **54**, 149 (2001).
41. P. Banerjee, D. J. Irvine, A. M. Mayes, L. G. Griffith, *J. Biomed. Mater. Res.* **50**, 331 (2000).
42. The authors acknowledge contributions to this work from A. Briggs, D. Bucknall, V. Burlakov, J. Czernuska, and S. Wilkinson from Oxford University; N. Marston and I. Robinson from Lucite International; and Y. Tsukahara from the Toppan Printing Company.

VIEWPOINT

20th- to 21st-Century Technological Challenges in Soft Coatings

Robert R. Matheson Jr.

Coatings are among the most ancient technologies of humankind. Relatively soft coatings comprising organic materials such as blood, eggs, and extracts from plants were in use more than 20,000 years ago, and coating activity has been continuously practiced since then with gradually improving materials and application techniques. The fundamental purposes of protecting and/or decorating substrates have remained ubiquitous across all the centuries and cultures of civilization. This article attempts to extrapolate the long tale of change in soft coating technology from its current state by identifying some key problems that attract research and development efforts as our 21st century begins.

Humans have been decorating and protecting various surfaces for many thousands of years. One very useful way of accomplishing either or both of those tasks is to apply a thin layer of some new material with appropriate char-

acteristics (of appearance, durability, adhesion, and application requirements) directly onto the surface of interest. That new material is a coating. Understandably, the early history of coatings is a story of very specialized,

often unique material combinations, as trial and error achieved goals with only the materials at hand in nature. This heritage of customization is still detectable in the modern coatings world, which demands a tremendous amount from the materials—often synthetic but some still containing or made of natural products—to be thinly applied on a surface. They need to be easily and uniformly applied; set up within a reasonable amount of time and process constraints; have a minimal environmental impact in their synthesis, combina-

DuPont Performance Coatings, 950 Stephenson Highway, Troy, MI 48063, USA. E-mail: robert.r.matheson@usa.dupont.com